Freezing of dimers on a square lattice: a finite-size-scaling study



1993 J. Phys. A: Math. Gen. 26 5255

(http://iopscience.iop.org/0305-4470/26/20/012)

J. Phys. A: Math. Gen. 26 (1993) 5255–5266. Printed in the UK

# Freezing of dimers on a square lattice: a finite-size-scaling study

G Fiumara† and P V Giaquinta‡

† Dottorato di Ricerca in Fisica, Università degli Studi di Messina, Casella Postale 50, Villaggio S. Agata, 98166 Messina, Italy

‡ Dipartimento di Fisica, Sezione di Fisica Teorica, Università degli Studi di Messina, Casella Postale 50, Villaggio S. Agata, 98166 Messina, Italy

Received 5 January 1993

**Abstract.** We present a Monte Carlo study of a classical lattice-gas Hamiltonian formerly introduced by Parrinello and Tosatti in order to describe the coexistence of atomic and molecular phases. The nature of the ordering transition undergone by the dense molecular fluid into a molecular-crystal phase is investigated in two dimensions through phenomenological finite-size-scaling techniques.

## 1. Introduction

Implementing a statistical-mechanical theory of the phase diagram of chemically reacting species poses rather severe problems which pertain, on one hand, to an adequate treatment of the molecular bond and, on the other, to a proper account of the role played by temperature and density on the outbreak of macroscopic coexistence of atomic and molecular phases. However, in order to acquire some feeling on the interplay between energy and entropy effects in this process, it is useful to investigate simple models suitably endowed with some of the key features that may be responsible for the above phenomenonology.

The lattice-gas Hamiltonian that is the object of the present study was in fact proposed by Parrinello and Tosatti (PT) to simulate the *saturation* of a diatomic bond through classical monatomic interactions [1]. For arbitrary space dimension the PT Hamiltonian reads [2]:

$$\mathcal{H} - \mu N = -(J/2) \sum_{(i,j)} \left[ \prod_{k(i)} (1 - c_k) \right] c_i c_j \left[ \prod_{l(j)} (1 - c_l) \right] - \mu \sum_i c_i \qquad (1)$$

where $(i, j)$ run over all pairs of nearest-neighbour sites in the lattice, $k(i)$ labels the first neighbours of site $i$ that are different from $j$, and, similarly, $l(j)$ labels the first neighbours of site $j$ different from $i$. The site-occupancy variable $c_i$ takes on the value zero or one for an empty or filled site, respectively, and thus determines the fluctuating number of occupied sites $N$ for a given value of the chemical potential $\mu$. The projectors that appear in the PT Hamiltonian on both sides of the Ising-type term $c_i c_j$ allow the formation of a bond between two neighbouring particles if and only if all of the residual nearest-neighbour sites are vacant. This constraint implies interactions that are clearly

0305-4470/93/205255+12$07.50  

non-local and irreducibly many-body. The binding energy resulting from the formation of a dimer is $-J$, with $J>0$.

From now on, we shall deal with the properties displayed by the PT Hamiltonian on a two-dimensional square lattice. In this geometry the generic interaction term in (1) involves up to eight sites simultaneously. At zero temperature, according to the value of the chemical potential, the model switches between three distinct ground states.

For $\mu<-\frac{1}{2}J$, the lattice is empty.

In the range $-\frac{1}{2}J<\mu<\frac{1}{2}J$ the minimum-energy configuration is that of a 'molecular crystal' (MC) made up by staggered rows of parallel dimers (see figure 1 of [3]). The resulting ground state, which can also be described as a close-packed structure formed by the hexagonal tiles corresponding to the exclusion shells of each dimer, is half-filled and eight-fold degenerate. In fact, the equilibrium MC state is a 'mixture' of translation-invariant 'pure states', four of which are transformed one into another by rigidly shifting dimers along the crystal polarization axis. The residual four states are equivalent to the former four ones but for the orientation of the PT dimers which, on a square lattice, may point along two orthogonal directions.

For $\mu>\frac{1}{2}J$, the ground state is a closest-packed atomic state in which particles fill up the whole lattice.

The marked difference between the lattice coverages realized in the molecular and atomic states is the result of the steric hindrance effect associated with the formation of an (elongated) chemical bond. Indeed, such effects turn out to be crucial in driving the dissociative molecular-to-atomic transition in real systems under high pressure.

For $T>0$, the formerly empty region becomes populated with particles that are mostly bonded and give rise to a fluid phase whose range of stability extends, with increasing temperatures, further and further beyond the ground-state threshold, $\mu=\frac{1}{2}J$. Correspondingly, the MC region shrinks (also on the high-density atomic 'side'), eventually collapsing onto one single end-point whose thermodynamic coordinates are $T_{MC}\simeq 0.3J/k_B$ (where $k_B$ is Boltzmann's constant) and $\mu_{MC}\simeq 0.27J$, respectively [2]. For $T>T_{MC}$, the sharp thermodynamic distinction between the disordered molecular and atomic phases fades out. Finer analysis reveals the persistence in the 'supercritical' fluid region of a *diffuse* dissociative transition that is signalled by the anomalous behaviour of the constant volume derivative of the pressure with respect to temperature [3]. This last quantity has been discussed in relation to the experimental evidence of a continuous dissociative transition in fluid nitrogen shock-compressed at high temperatures [4–6].

In this paper we present the first systematic finite-size-scaling analysis of the Monte Carlo ($\mathcal{MC}$) results obtained for the molecular freezing transition in the PT framework. The layout of the paper is as follows: In section 2 we discuss some methodological aspects concerned with the simulation algorithm which was implemented with the multiple-histogram technique of Ferrenberg and Swendsen [7, 8] in order to obtain, through one set of data collected for a given thermodynamic state, probability distributions at nearby values of temperature and chemical potential. The numerical results are presented in section 3 together with a finite-size-scaling analysis of the data. Section 4 is finally devoted to concluding remarks.

## 2. Simulation method

We performed standard $\mathcal{MC}$ simulations on square lattices with linear size $L=4n$ ($n\leqslant 8$), under periodic boundary conditions (p.b.c.). The PT Hamiltonian was sampled

along two isotherms corresponding to inverse temperatures $\tilde{\beta}=3.5$ and 4.0, respectively, where $\tilde{\beta}=\beta J$ (correspondingly, $\tilde{\mu}=\mu/J$). An $\mathcal{MC}$ move consisted of an attempt at removing an existing particle or at inserting a new one in an empty lattice site. The algorithm used was such that the molecular axis of dimers forming at equilibrium might indifferently align along any of the two allowed directions.

Following Ferrenberg and Swendsen [7], along each run we accumulated the histogram $\mathcal{N}_{(\beta,\mu)}(N, N_b)$, i.e. the number of configurations produced for each value of the number of particles $N$ and number of bonds $N_b=-E/J$ (where $E$ is the energy) in the thermodynamic state characterized by the parameters $\beta$ and $\mu$.

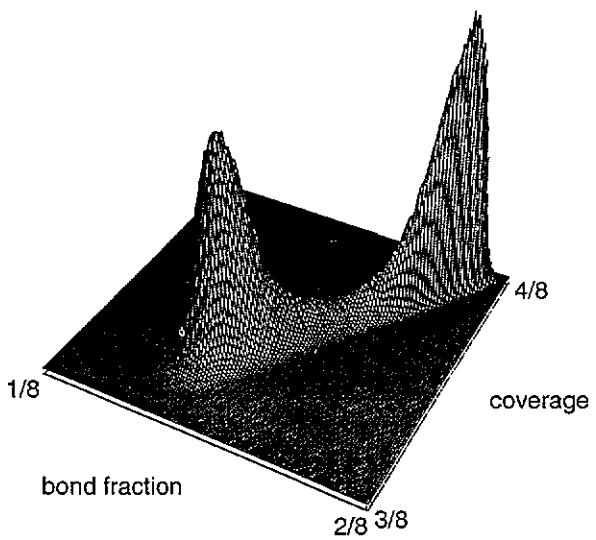


**Figure 1.** Three-dimensional plot of the histogram $\mathcal{N}_{(\beta,\mu)}(N, N_b)$ for a $32\times32$ lattice at $\tilde{\beta}=3.5$ and $\tilde{\mu}=0.156$.

Histograms were updated after a sweep over the lattice. Figure 1 shows a three-dimensional plot of such a histogram for a state corresponding to a molecular liquid close to the freezing point. The two-peak surface stretches along a straight line $N=2N_b+\alpha(L^2-4N_b)$, the excess of $N$ with respect to $2N_b$ corresponding to monomers or particles bunched in clusters. The value of the positive quantity $\alpha$ depends on the state parameters $\beta$ and $\mu$. Liquid-like configurations give rise to the front hill whose maximum in figure 1 happens to lie at a point with coordinates $N_b/L^2\simeq0.18$ and $N/L^2\simeq0.41$. The shape of this hill is systematically more rounded than that of the ridge resulting from ordered 'crystal' states which, instead, looks thinner and rather elongated.

The evolution of the reduced histogram obtained after resumming $\mathcal{N}_{(\beta,\mu)}(N, N_b)$ over $N$ is presented in figure 2: the change in the relative weights of the two maxima monitors the transition from the molecular-liquid to the molecular-crystal state.

Equilibrium averages were computed as

$$\bar{\mathcal{X}}(\beta,\mu)=\frac{1}{\hat{\mathcal{N}}(\beta,\mu)}\sum_{N,N_b}\mathcal{N}_{(\beta,\mu)}(N, N_b)\mathcal{X}(N, N_b) \qquad (2a)$$

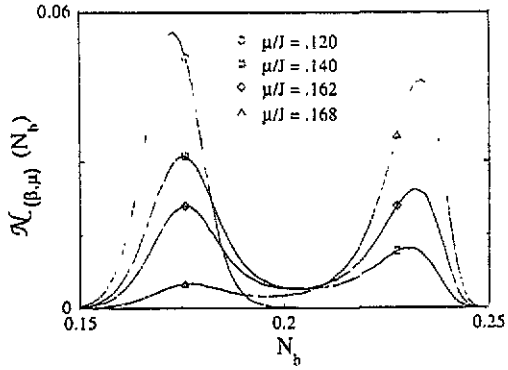


**Figure 2.** Reduced histograms of states $\mathcal{N}_{(\beta,\mu)}(N_b) \equiv [\hat{\mathcal{N}}(\beta,\mu)]^{-1} \sum_N \mathcal{N}_{(\beta,\mu)}(N, N_b)$ for a $32 \times 32$ lattice at $\tilde{\beta} = 3.5$ plotted for a number of values of the chemical potential referring to states on both sides of the transition point.

where

$$\hat{\mathcal{N}}(\beta, \mu) \equiv \sum_{N,N_b} \mathcal{N}_{(\beta,\mu)}(N, N_b). \tag{2b}$$

In our runs, the value of this quantity ranged between $4 \times 10^5$ and $4 \times 10^6$ $\mathcal{MC}$ configurations per site.

In order to perform a finite-size-scaling analysis of the $\mathcal{MC}$ data across the transition with sufficient reliability and confidence, one needs to resolve with great precision the shape of the maxima (i.e. their height, half-width, and position) which typically show up in the thermodynamic response functions. To this aim, we resorted to the multiple-histogram technique as implemented by Ferrenberg and Swendsen [8]. The data obtained through the equilibrium sampling performed on a grid of points along each isotherm were combined so as to obtain an optimized estimate for the density of states in the form of a continuous function.

The quantities evaluated during each run were the average number of bonds per site $\Theta_b \equiv \bar{N}_b / L^2$ and the total fractional coverage $\Theta \equiv \bar{N}/L^2$ together with the $2 \times 2$ matrix of the second-order correlation moments $\mathcal{I}_{ij} \equiv \Delta\mathcal{X}_i \Delta\mathcal{X}_j$, where $\Delta\mathcal{X}_i \equiv \mathcal{X}_i - \bar{\mathcal{X}}_i$ is the fluctuation of the extensive property $\mathcal{X}_i$ (energy, number of particles) about its average value. We recall that the thermodynamic-fluctuation theory leads to the following relations [9]:

$$\mathcal{I}_{11} \equiv \overline{(\Delta E)^2} = -\left.\frac{\partial \bar{E}}{\partial \beta}\right|_{\beta\mu} \tag{3a}$$

$$\mathcal{I}_{12} \equiv \overline{(\Delta E \Delta N)} = \left.\frac{\partial \bar{E}}{\partial \beta \mu}\right|_{\beta} \tag{3b}$$

$$\mathcal{I}_{22} \equiv \overline{(\Delta N)^2} = \left.\frac{\partial \bar{N}}{\partial \beta \mu}\right|_{\beta} \tag{3c}$$

where the 'volume' is tacitly kept fixed in each derivative. Obviously, the two off-diagonal elements are equal and consistently verify the appropriate Maxwell relation.

## 3. Results

### *3.1. Monte Carlo data*

We start by showing how typical averages computed through (2) on a discrete mesh of points compare with the corresponding estimates obtained over a continuous range

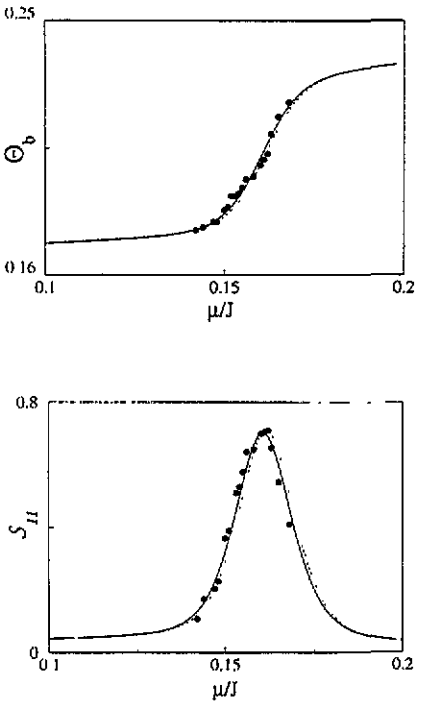


**Figure 3.** Average bond fraction $\Theta_b$ and corresponding second-order correlation moment $\mathscr{I}_{11}$ for a $32 \times 32$ lattice at $\tilde{\beta} = 3.5$: solid circles, $\mathscr{MC}$ data; dashed lines, single-histogram estimate based on the $\mathscr{MC}$ data for $\tilde{\mu} = 0.16$ only; continuous lines, results of the multiple-histogram method implemented with the data relative to 16 states in the range $0.14 \leqslant \tilde{\mu} \leqslant 0.168$.

of values via both the single- and multiple-histogram techniques. Figure 3 shows the average number of bonds (energy) per site and the first diagonal term of the fluctuation matrix. This quantity may be related to the ordinary specific heat $C$ that is computed after keeping both the volume and the average number of particles $\bar{N}$ constant. In fact, upon reducing the derivative that appears in (3*a*) to the form where the extensive variable $\bar{N}$ is kept fixed instead of the conjugate intensity $\beta\mu$, we find

$$\frac{1}{\beta^2}(C/k_B) = \mathscr{I}_{11} - \mathscr{I}_{12} \cdot \mathscr{I}_{22}^{-1} \cdot \mathscr{I}_{21}. \tag{4}$$

As is clearly seen from figure 3, the estimate obtained by extending the information contained in one single histogram (which, in figure 3(*b*), is the one produced for a

value of the chemical potential corresponding to the position of the maximum) already provides a fair, overall agreement with the $\mathcal{MC}$ data. However, the multiple-histogram implementation of the Ferrenberg–Swendsen technique does visibly improve upon the single-histogram result, ultimately furnishing a smooth and accurate interpolation of the data points. This feature is indeed preserved (with a comparable level of accuracy) for all of the sizes that we have explored.

The size dependence of the average quantities $\Theta$ and $\Theta_b$ and of the three second-order correlation moments $\mathcal{S}_{ij}$ is shown in figures 4 and 5, respectively, for $\tilde{\beta}=3.5$. It

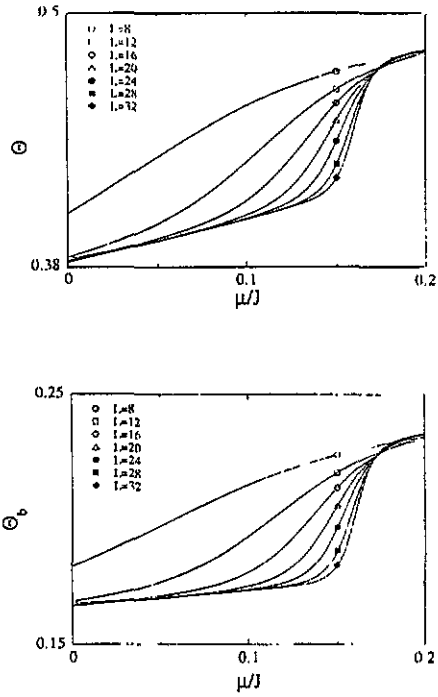


**Figure 4.** Size dependence of the fractional coverage $\Theta$ and average bond fraction $\Theta_b$ plotted as a function of the chemical potential for $\tilde{\beta}=3.5$.

is apparent that, as $L$ increases, the variation of the bond and number density profiles as a function of the chemical potential becomes more and more abrupt. We also note that, upon enlarging the size of the lattice, spurious coherence effects associated with p.b.c.—which, to some extent, concur in anticipating the formation of the long-range-ordered phase—are progressively depressed. Correspondingly, the location of the maximum in the thermodynamic response functions shifts to greater values of the chemical potential, which indicates that a closer packing of dimers is needed in order to drive the transition towards the crystalline phase.

### *3.2. Finite-size scaling*

The conventional route followed for determining the character of a phase transition blowing up in a finite system is to study how the thermodynamic response functions scale with the size of the lattice. In fact, it is well known that any jump or singularity associated with a sharp change of state occurring in the thermodynamic limit is smeared

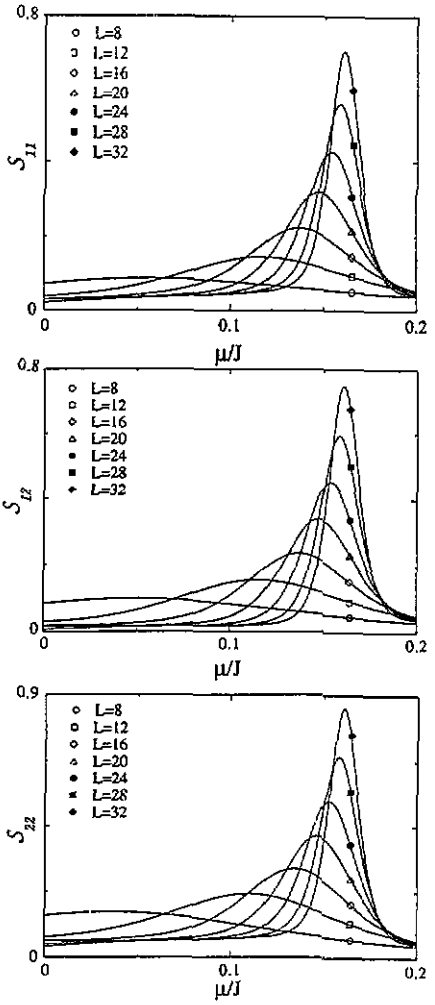


**Figure 5.** Size dependence of the three second-order correlation moments plotted as a function of the chemical potential for $\beta = 3.5$.

out in a finite system: as a result, one observes a rounding and, possibly, also a shifting of the transition over some region of the equilibrium parameters. It is through an analysis of such asymptotic finite-size effects that one may ultimately ascertain the continuous or discontinuous nature of the transition.

The theory of finite-size scaling at critical points is firmly settled [10, 11], while a corresponding framework for dealing with first-order transitions has been formulated only rather recently [12]. The scaling of both symmetric and asymmetric first-order phase transitions is now fairly well understood [13–19]. We recall that first-order transitions driven by an internal thermodynamic field (such as the temperature or, as in the present case, also the chemical potential) are normally asymmetric. A phenomenological mean-field-type approach for dealing with such transitions in a finite system was first pursued by Challa and co-workers who described the co-existing phases by Gaussian distributions with the same height [16]. Later studies, based on a more rigorous statistical-mechanical basis [17–19], proved that this assumption was incorrect and

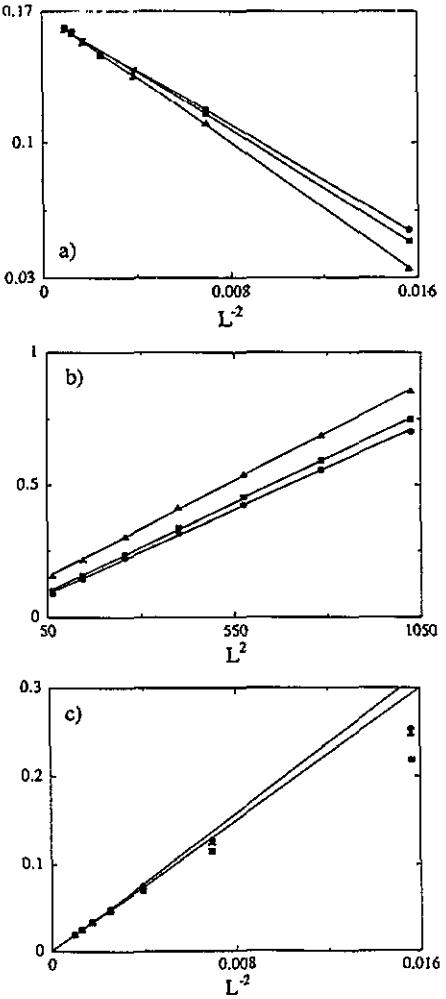


**Figure 6.** Position (a), height (b), and half-width (c) of the thermodynamic response functions as a function of the lattice size for $\tilde{\beta}=3.5$: circles, squares, and triangles refer to $\mathscr{I}_{11}$, $\mathscr{I}_{12}$, and $\mathscr{I}_{22}$, respectively. The continuous lines represent linear-regression fits of the data. As is seen from (c), the half-widths approach their asymptotic scaling behaviour more slowly than the other two indicators. The corresponding regression lines were in fact traced using the data for $L \geqslant 20$.

showed that it is not the heights but the volumes underneath the peaks that become equal at the transition [17]. Notwithstanding the wrong assumption made by Challa and co-workers, the corrected theory—which has been successfully tested against the $\mathscr{MC}$ data for the ten-state Potts model in two dimensions [20, 21]—still confirmed one central conclusion reached in [16] on the general scaling behaviour that should be expected on a $d$-dimensional lattice with p.b.c. at a point of multiple-phase co-existence: i.e. a rounding and shifting of leading order $L^{-d}$. By contrast, at a second-order transition such effects are controlled by a diverging correlation length and do typically scale as $L^{-1/\upsilon}$, where $\upsilon$ is the correlation-length critical exponent.

In order to identify the nature of the molecular freezing transition exhibited by the PT model, we now investigate how the position, height and half-width of the peaks

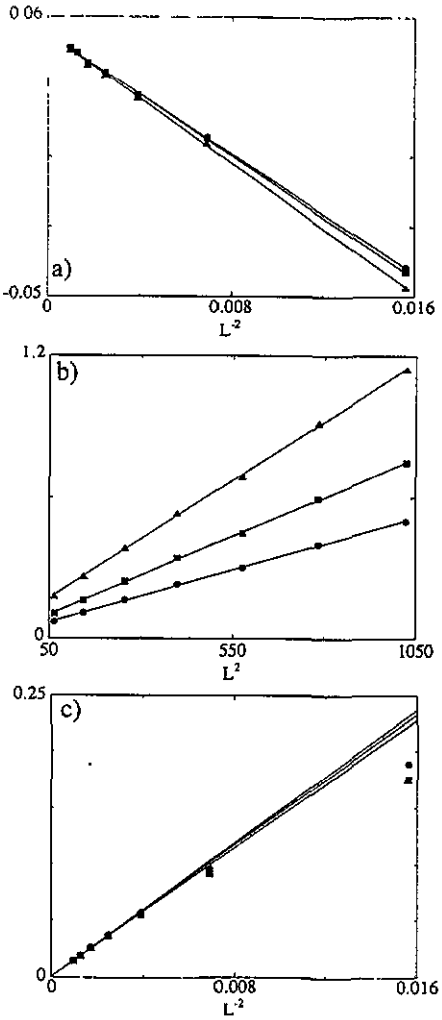


**Figure 7.** Position (a), height (b), and half-width (c) of the thermodynamic response functions as a function of the lattice size for $\tilde{\beta}=4.0$. The meaning of the lines and symbols is the same as in figure 6.

exhibited by the second-order fluctuation moments change as a function of the lattice size along two distinct isotherms ($\tilde{\beta}=3.5$, 4.0) which extend across the transition line. The finite-size-scaling analysis was carried out on the analytical 'representations' of the $\mathcal{MC}$ data synthetically provided by the multiple-histogram technique discussed above.

The results of this analysis are presented in figures 6 and 7. These plots clearly show that all the chosen indicators scale as $L^{-2}$ (or its reciprocal), the expected marker—apart from lower-order corrections—of a first-order phase transition in two dimensions. The 'quality' of the asymptotic linear behaviour shown by each of the above indicators was also tested through a three-parameter fit of the form $\rho L^{\sigma}+\tau$: the results did indeed confirm a direct or reciprocal dependence upon $L^{-2}$.

As a byproduct of the analysis, we obtain the 'infinite-size' estimate of the chemical potential at the transition point $\tilde{\mu}^{c}_{\infty}$ (in units of $J$) as a function of the temperature.

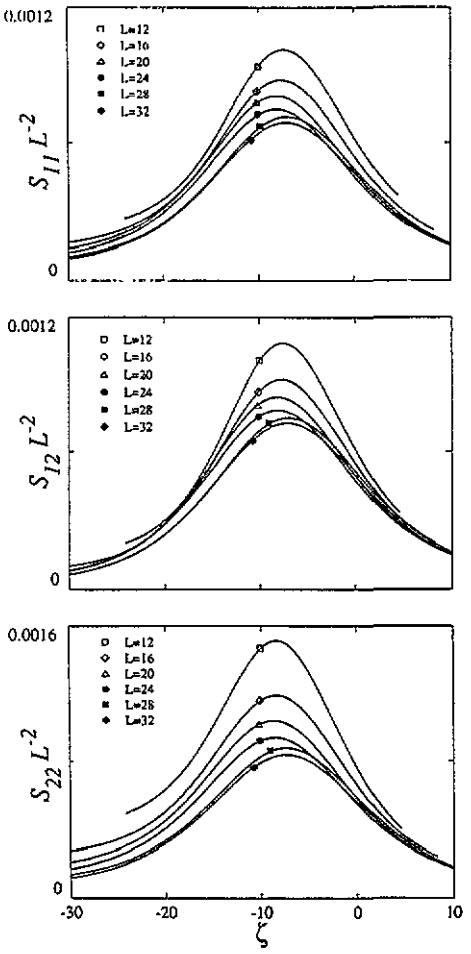


**Figure 8.** Second-order correlation moments $\mathscr{S}_{ij}(\beta, \mu; L)$ divided by $L^2$ plotted as a function of $\zeta = [\tilde{\mu} - \tilde{\mu}^c_\infty(\beta)]L^2$ for $\tilde{\beta} = 3.5$.

For $\tilde{\beta} = 3.5$ we find $\tilde{\mu}^c_\infty = 0.167$–$0.168$, while for $\tilde{\beta} = 4$ the transition point shifts to $\tilde{\mu}^c_\infty = 0.053$.

The finite-size-scaling theory also implies that at a first-order phase transition the reduced specific heat $C_L L^{-2}$ is a scaling function of $(T - T^c_\infty)L^2$, where $T^c_\infty$ is the bulk critical temperature [16, 20]. A test of this statement for the correlation moments $\mathscr{S}_{ij}(\beta, \mu; L)$ is presented in figure 8. The shifts of the peak positions $\mu^{max}_{ij}(\beta; L)$ in the finite system show up in figure 8 as a displacement of the maxima from the origin to the values $[\mu^{max}_{ij}(\beta; L) - \mu^c_\infty(\beta)]L^2$.

In order to estimate the coverage and energy jumps at the transition we have also studied the size-dependence of the points of maximum curvature in the particle and bond-density profiles. From equations (3*b*) and (3*c*) it follows that these points do also correspond to the pair of inflection points that bracket the maximum in $\mathscr{S}_{12}$ and $\mathscr{S}_{22}$ plotted at constant temperature as a function of $\mu$. As shown in figure 9, the values of $\Theta$ and $\Theta_b$ at such two points scale linearly as a function of $L^{-2}$. We find that a linear

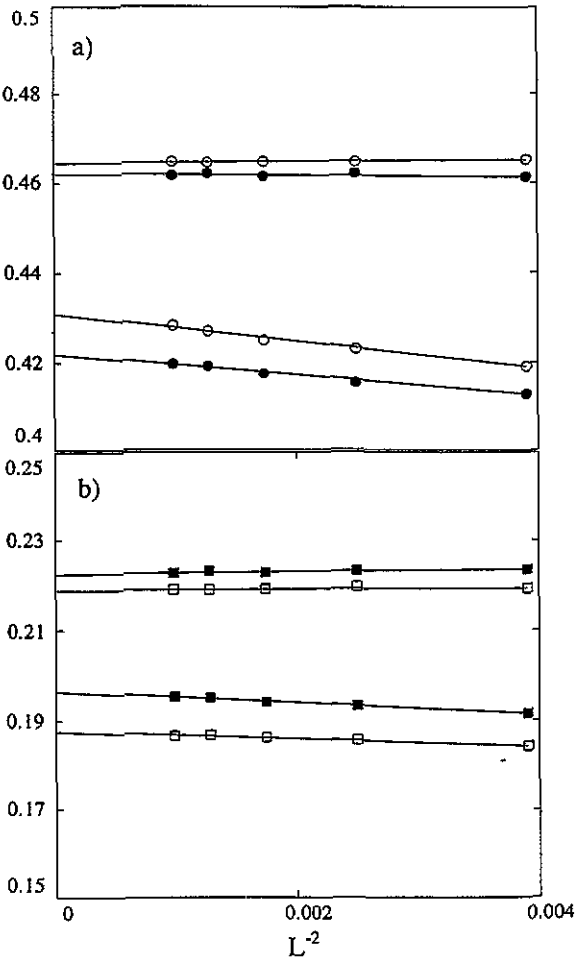


**Figure 9.** Points of maximum curvature in the particle and bond-density profiles plotted as a function of $L^{-2}$: circles (a) and squares (b) refer to $\Theta$ and $\Theta_b$, respectively, for $\tilde{\beta}=3.5$ (open symbols) and $\tilde{\beta}=4.0$ (solid symbols). The continuous lines represent linear-regression fits of the data.

**Table 1.** Estimated jumps of the bond and number coverage at inverse temperatures $\tilde{\beta}=$ 3.5 and 4.0. The resulting discontinuity in the entropy per site $s$ (in units of $k_B$) is also reported.

| $\tilde{\beta}$ | $\Delta\Theta_b$ | $\Delta\Theta$ | $\Delta s$ |
|---|---|---|---|
| 3.5 | 0.0313 | 0.0335 | −0.1291 |
| 4.0 | 0.0260 | 0.0402 | −0.1126 |

regression of the data yields *different* values for the asymptotic densities that correspond to the points of maximum curvature in both the coverage and bond fraction profiles at each temperature. In table 1 we report the extrapolated jumps together with the resulting discontinuity in the entropy of the lattice.

## 4. Conclusions

In this paper we have discussed the results of a finite-size-scaling analysis carried out for a rather complex lattice-gas Hamiltonian which was devised in order to mimic the saturation of a molecular bond by means of classical, non-local interactions [1–3]. The model was sampled on a two-dimensional square lattice through extensive Monte Carlo simulations implemented with the multiple-histogram technique proposed by Ferrenberg and Swendsen [7, 8].

For small values of the chemical potential, the phase diagram implies the existence of a fluid of diatomic molecules in equilibrium with a dilute gas of monatomic particles. Below a 'critical' temperature $T_{MC} \simeq 0.3J/k_B$, upon increasing the value of the chemical potential, this fluid freezes into an ordered phase. The present $\mathscr{MC}$ simulations carried out for different lattice sizes and analysed through finite-size-scaling techniques provide convincing evidence that the molecular freezing transition, as decribed by the Parrinello and Tosatti Hamiltonian, is thoroughly first order.

## Acknowledgments

This work has been supported by the Ministero dell'Università e della Ricerca Scientifica e Tecnologica and by the Consorzio Interuniversitario Nazionale di Fisica della Materia.

## References

[1] Parrinello M and Tosatti E 1982 *Phys. Rev. Lett.* **49** 1165
[2] Florio G M, Giaquinta P V, Parrinello M and Tosatti E 1984 *Phys. Rev. Lett.* **52** 1899
[3] Giaquinta P V and Giunta G 1989 *Phys. Rev.* B **39** 4716
[4] Nellis W J, Holmes N C, Mitchell A C and van Thiel M 1984 *Phys. Rev. Lett.* **53** 1661
[5] Radousky H B, Nellis W J, Ross M, Hamilton D C and Mitchell A C 1986 *Phys. Rev. Lett.* **57** 2419
[6] Nellis W J, Radousky H B, Hamilton D C, Mitchell A C, Holmes N C, Christianson K B and van Thiel M 1991 *J. Chem. Phys.* **94** 2244
[7] Ferrenberg A M and Swendsen R H 1988 *Phys. Rev. Lett.* **61** 2635
[8] Ferrenberg A M and Swendsen R H 1989 *Phys. Rev. Lett.* **63** 1195
[9] Callen H B 1985 *Thermodynamics and an Introduction to Thermostatistics* (New York: Wiley)
[10] Fisher M E 1971 *Critical Phenomena* M S Green ed (New York: Academic)
[11] Barber M N 1983 *Phase Transitions and Critical Phenomena* vol 8 C Domb and J L Lebowitz eds (New York: Academic Press)
[12] For an extended discussion see, for instance, the collection of reviews: *Finite-Size scaling and Numerical Simulations of Statistical Systems* V Privman ed 1990 (Singapore: World Scientific)
[13] Privman V and Fisher M E 1983 *J. Stat. Phys.* **33** 385
[14] Binder K and Landau D P 1984 *Phys. Rev.* B **30** 1477
[15] Fisher M E and Privman V 1985 *Phys. Rev.* B **32** 447
[16] Challa M S S, Landau D P and Binder K 1986 *Phys. Rev.* B **34** 1841
[17] Privman V and Rudnik J 1990 *J. Stat. Phys.* **60** 551
[18] Borgs C and Kotecky R 1990 *J. Stat. Phys.* **61** 79
[19] Borgs C, Kotecky R and Miracle-Sole S 1991 *J. Stat. Phys.* **62** 529
[20] Lee J and Kosterlitz J M 1991 *Phys. Rev.* B **43** 3265
[21] A further extension of the theory has been recently applied to the three-state Potts ferromagnet in three dimensions by Vollmayr K, Reger J D, Scheucher M and Binder K 1993 *Z Phys.* B **91** 113